Removal of Trinitrotoluene Traces from Water using Graphene Oxide Nanosheets

Waleed F. Khalil¹, Salah Tolba², M. A. Mahmoud², AE. Elbeih², H. E. Mostafa²

¹ Safety Fuel Cycle Department, Nuclear and Radiological Safety Research, Egyptian Atomic Energy Authority (EAEA). Cairo, Egypt

Corresponding author: waleed_fekry12878@yahoo.com

Abstract. Water pollution has consistently been an issue for the environment. TNT is commonly found in soil, groundwater, and surface water near manufacturing facilities due to inadequate disposal practices. The environmental permanence and human exposure to TNT degradation products are issues of concern. TNT endures because of inadequate biodegradation and photolysis rates. A multitude of scientists are exploring nanomaterials as a solution to this issue. Graphene oxide (GO) is one of the important carbon materials that can be used to remove traces of trinitrotoluene due to having several oxygen functional groups. Herein, the prepared Graphene oxide using the improved hammer method was applied to remove TNT residue from water. The as-synthesized GO was characterized by XRD, FTIR, and SEM. The as-prepared GO was applied as an adsorbent to remove TNT from water. Removal studies of trinitrotoluene were carried out using (HPLC). The effect of contact duration, pH, and temperature on adsorption has been examined. The findings revealed that the peak adsorption capability for GO was approximately 180.8 mg/g. We concluded that a pH of around 6 and a temperature of around 35 °C are optimal conditions for the elimination of TNT from water. The result indicated that the efficiency of removal exceeded 90.0%.

Keywords: Trinitrotoluene Traces; Graphene Oxide; Wastewater Treatment.

² Military Technical College (MTC), Kobry Elkobbah, Cairo, Egypt

1-Introduction

Water is now one of the most vital resources, possessing economic, social, political, and environmental significance globally. In recent years, water contamination has emerged as a critical environmental concern, garnering global attention due to swift industrial growth that has brought several contaminants into aquatic habitats. [1]. Remediation of polluted sites is necessary due to the toxicity of most contaminants. 2,4,6-trinitrotoluene (TNT) and crude oil were studied as high-priority pollutants. TNT was the predominant explosive used during the 20th century. Continuous pollution has generated an urgent requirement for treatment. 7, 5, 7 trinitrotoulene (TNT) was the preferred explosive in World Wars I and II due to its low cost, safety, and low impact sensitivity. Thus, TNT remnants from war grounds and ammunition factories pollute land and groundwater globally. TNT is poisonous and mutagenic, making contaminated places dangerous. Thus, TNT remediation in contaminated locations is crucial. Bioremediation, incineration, photodegradation, and adsorption are the most investigated remediation strategies. Adsorption can treat stubborn, harmful organic contaminants in water and soils on a massive scale [Y]. TNT, or 2,4,6-trinitrotoluene, is a highly potent explosive used for industrial and military applications. To make conventional TNT in weapons and military facilities, toluene is nitrated, and then crude TNT is washed with hot water and sodium sulfite baths. "TNT red water" is the name for the very bright red liquid that is released when you wash clothes. It is mostly made up of TNT, MNT, DNT, DNTS, acidic residues, and other nitroaromatic substances [3, 4]. Nitroaromatic compounds constitute the primary components of TNT red water, exhibiting resistance to biodegradation, This causes these dangerous stubborn contaminants to build up in the environment. The U.S. Environmental Protection Agency has classified TNT red water as hazardous waste under the Resource Conservation and Recovery Act (RCRA) due to its demonstrated toxicity to organisms. Both terrestrial and marine ecosystems face significant threats from directly discharging untreated TNT red water into the environment. Consequently, before the discharge of TNT red water into the soil or aquatic environments, it must undergo thorough treatment, particularly to eliminate the explosive pollutant TNT. Nonetheless, due to the toxicity of TNT to facultative, anaerobic, and aerobic microorganisms. the biodegradation of TNT red water has exhibited minimal efficacy [5]. TNT and DNT in red water are broken down by immobilised microbial technology, according to Zhang et al. (2015). The polyammoniacum foaming carrier improved mass transfer kinetics and immobilised microorganisms by increasing surface area. Because commercially available activated carbon has poor adsorption and regeneration capacities, it is unable to extract TNT from water [6]. The ecology is affected when used activated carbon is disposed away, and if the adsorbent is not reusable, this treatment procedure will be quite expensive. When wastewater contains modest levels of TNT (less than 60 mg L-1), The GAC is ineffective. The effectiveness of a GAC-based adsorption system is limited by the amount of TNT and its byproducts present in TNT red water, which can reach up to 800 mg L-1. Cu-impregnated activated coke (CAC) removed 85.34% of the COD in TNT red water [7].

The aquatic plant Ambrosia trifida produces biochar, which has demonstrated significant effectiveness in cleaning up aqueous TNT. The approach attained an equilibrium adsorption capacity of 76.9 mg/g. Significant adsorption and regeneration capacities have been shown by graphene-based adsorbents in the treatment of water contaminated with TNT. The interaction between the electrophilic TNT molecule and nucleophilic sites in the adsorbent is improved by the intercalation of metal ions [8]. Yadav et al. (2024) used graphene nanocomposites made of graphite and sludge to extract TNT from red water. Iron intercalation produced multilayered, high-surface-area, and highly microporous graphene nanocomposites. The graphene nanocomposites produced from sludge exhibited a surface area of 748 m² g⁻¹ and a pore volume of 0.55 cm³ g⁻¹. TNT red water had an absorption capacity of 151.6 mg g⁻¹ due to these properties. Graphene nanocomposite serves as a cost-effective, recyclable, and reusable adsorbent for the treatment of TNT red water [3]. The intraparticle diffusion process predominantly governs the adsorption mechanism, with reduced graphene oxide (rGO) augmented by nano zero-valent iron (nZVI) exhibiting an adsorption capacity of 41.9 mg g⁻¹ for TNT from an aqueous solution [9].

The purpose of this work was to use the enhanced hammer method to manufacture graphene oxide nanosheets. FTIR, SEM, and XRD were used to characterise the produced graphene. The adsorption characteristics for the treatment of TNT were examined using the as-prepared graphene oxide nanosheets. High-performance liquid chromatography (HPLC) was used to quantify the residue content of TNT before to and post to its adsorption onto graphene nanosheets.

2. Materials and method

2.1. Materials

The study utilized graphite powder, potassium permanganate, sulphuric acid, phosphoric acid, hydrogen peroxide, nitric acid, hydrochloric acid, ethanol, methanol, and sodium hydroxide, with ultra-pure water and 2,4,6-trinitrotoluene supplied.

2.2 Preparation of graphene oxide

In 2022, Waleed F. Khalil et al. described an enhanced Hummers' process for synthesising graphene oxide from graphite powder [10]. To oxidise GO, the following techniques were used: a) Concentrated H2SO4 and H3PO4 (in a 2:1 ratio) were used to oxidise graphite in a sub-zero Celsius atmosphere while vigorously stirring the mixture. KMnO4 (18 g per 3 g of graphite) was then added progressively to the mixture. b) After adding the oxidised GO suspension to cold water with 30% H2O2, the water was exfoliated with ultrasonic vibrations. Centrifugation was used to wash graphene oxide many times using deionised water and 10% hydrochloric acid. d) The resultant graphene oxide was vacuum-dehydrated at 60 degrees Celsius.

2.3. Characterize of prepared GO

The ATR technique (PerkinElmer, Spectrum 2, USA) was employed to characterize the FTIR spectra of GO, TNT, and TNT/GO. It was determined to analyse each spectrum utilizing a Shimadzu X-ray diffractometer with a copper radiation wavelength of 1.54056 Å to enhance comprehension of the connection between graphite and graphene oxide. This experiment used Transmission Electron Microscopy (TEM) with a JEOL-JEM 2100 instrument manufactured in Japan. The surface morphology was analysed with the ZEISS EVO-MA10 scanning electron microscope.

2.4. Batch adsorption experiments

We conducted adsorption assays using 250 mL council flasks, following the steps below: We utilized a stock solution of 0.25 g for all adsorption tests during the research of GO (adsorbent) in deionized water. To prepare the adsorbate, 1.0 L of deionized water was included in the adsorbate stock solution. Standard TNT solutions with concentrations of 10, 25, 50, and 100 ppm were prepared by dilution. After two hours of stirring at 175 rpm, the adsorption suspension was centrifuged for 20 minutes at 5000 rpm. By deducting the equilibrium concentration (Ce) from the initial concentration (Co), we were able to determine the amount of TNT adsorbed on the GO. By computing the adsorption capacity and adsorption percentage using equations 1 and 2, we were able to ascertain the adsorption capacity.

Adsorption
$$\% = \frac{C_o - C_e}{C_o} \times 100\%$$
 (1)

Adsorption capacity =
$$\frac{C_o - C_e}{C_e} \times \frac{V}{m}$$
 (2)

 $C_{\rm o}$ (mg/L) and Ce (mg/L) provide the initial and equilibrium cobalt concentrations. The measures of the suspension (g) are volume V (ml) and adsorbent m (g). The average of at least three separate experiments is used for all of the data.

2.5. Sample analysis

To get rid of the GO suspension, all liquid samples were passed through MCE membrane filters with a pore size of $0.2 \,\mu m$. The methodology was adapted from EPA Method 8330 (USEPA, 1994). An HPLC

system (Agilent Infinity 1260) was used to measure the TNT concentration. A diode array detector (DAD) was used for detection, at detect TNT, the detector was adjusted at 240 nm. At a flow rate of 1.0 mL/min, we employed an isocratic combination of acetonitrile and water (50:50, v/v%). A C-18 reverse phase HPLC column of 15 cm x 4.6 mm and 5 μ m (Zorbax Eclapis) was filled with aliquots of 2 μ L [11].

3. Results and discussion

3.1. Characterization of graphene oxide

XRD investigations of graphite powder were conducted using graphite oxidation procedures, both before to and following oxidation. Graphite powder with a d-spacing of 3.34 displays a prominent peak at 2 theta = 26.1695°, as seen in Figure 1a. Upon the oxidation of graphite sheets, a new graphene oxide peak emerged at 2-theta = 10.93°, displacing the graphite peak. Functional groups intercalated between the graphite layers elevated the d-spacing value to 8.0427. This was elucidated by the significant oxidation of graphite utilized to generate graphene oxide. These findings correspond with other studies [12, 13]. Figure 2b shows an image of graphene oxide taken using transmission electron microscopy (TEM). The surface of the multilayer graphene oxide structure is smooth and transparent, with only little creases and wrinkles visible. You can see the FT-IR spectra of GO in Figure 1c. The FT-IR spectra of GO reveal an abundance of oxygen-containing functional groups. In C-C and C-C molecules, they are associated with the O-H and COOH bonds, whereas in C-O and C-OH bonds, they are related to the stretching vibrations. The graphene oxide surface was successfully created, according to the FTIR measurements [14]. One essential tool for characterising graphene oxide (GO) is Raman spectroscopy. Data from the Raman spectra are shown in Figure 1d. Two distinct bands were visible in the Raman spectroscopy of GO: found in 1597 cm-1 and 1345 cm-1, respectively, constitute the G-band. The intensity ratio (ID/IG) of the D and G bands was 0.842. The results are consistent with those of previous research [15].

3.2. Adsorption studies

3.2.1 Effect of TNT concentration. The adsorption capacities of a 0.5 g/L adsorbent at a constant pH of 6 and a temperature of 25 °C were evaluated with TNT concentrations of 10, 25, 50, and 100 ppm. The adsorption capacity of GO for TNT rises from 19.8 mg/g at 10 ppm to 134 mg/g at 100 ppm, as illustrated in Figure 3a. The adsorption capacity increases with rising TNT concentration due to the increased competition among TNT molecules for active sites on graphene oxide (GO). As the concentrations of these TNT compounds increase, the pulling force of the concentration gradient is enhanced. The adsorption surface initially is extensive, but it progressively diminishes as adsorption occurs and equilibrium is reached. The GO surface possesses a significant quantity of unoccupied active sites accessible for adsorption during the initial phase; however, it subsequently becomes increasingly difficult to occupy the remaining unfilled sites [16].

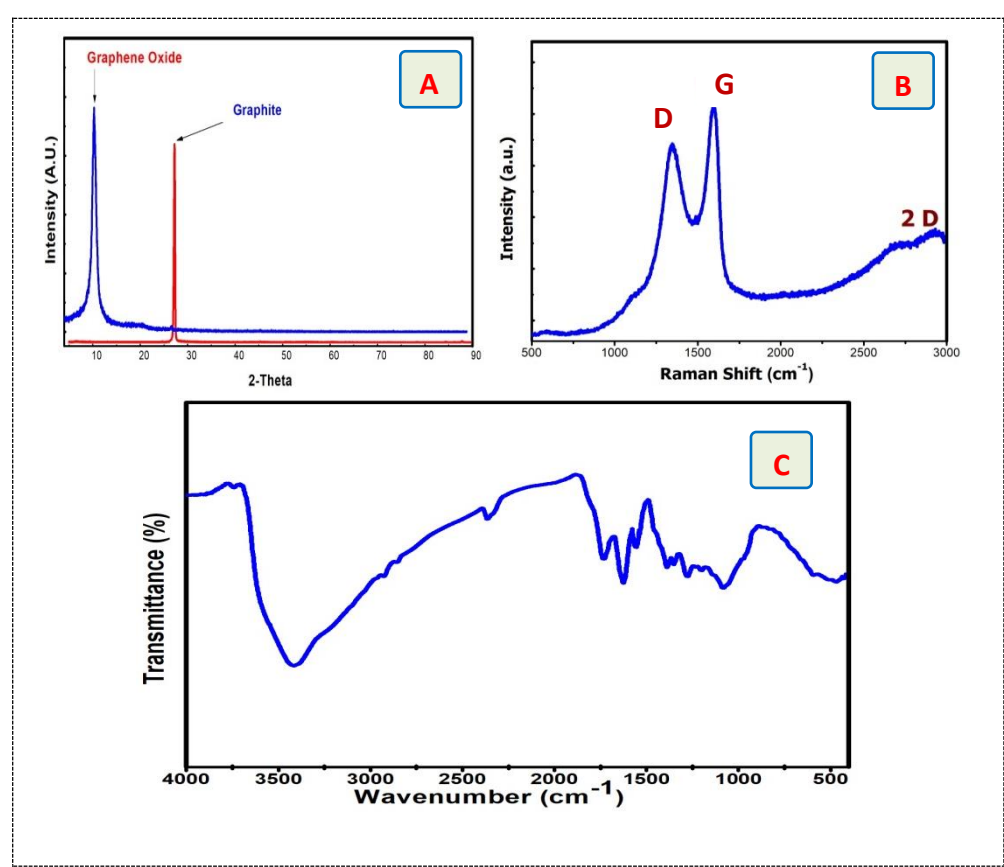


Figure 1. XRD patterns of GO and Graphite (a), Raman spectra of GO (b), HRTEM image of pure GO (c), FTIR spectra of graphene oxide pure

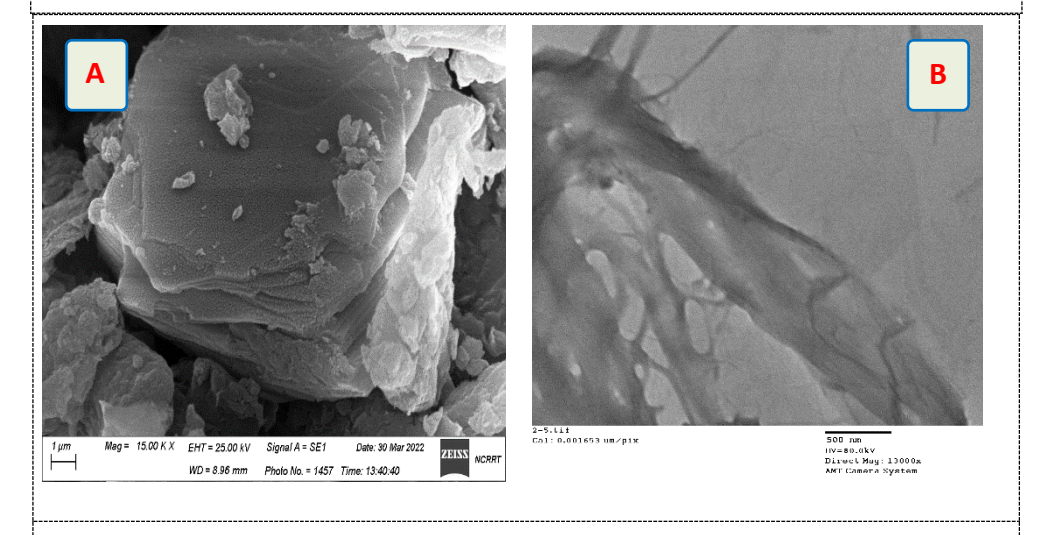


Figure 2. a) SEM image and b)TEM image of graphene oxide pure

3.2.2 Effect of temperature

The adsorption process was conducted at varying temperatures (25, 35, and 45 °C) at the prescribed conditions (0.5 g/L adsorbent, 100 ppm, and pH 6), as illustrated in Figure 5a, to optimize the parameters for TNT removal from the solution. Upon elevating the temperature from 25 to 35 degrees Celsius, the TNT adsorption capacity on GO augmented from 180.8 to 196.1 mg/g. Upon heating to 45 degrees Celsius, the adsorption capacity decreases to 146.4 particles per gram. At 35°C, an increase in adsorption capacity indicated that TNT exhibited an endothermic response to the GO surface. Moreover, the enhancement of more active sites has been associated with the temperature on the opposite side is 45°C. The increased mobility at elevated temperatures likely accounts for the reduction in TNT removal. Electrostatic interactions and surface complexation may diminish at temperatures over 45 degrees Celsius [17].

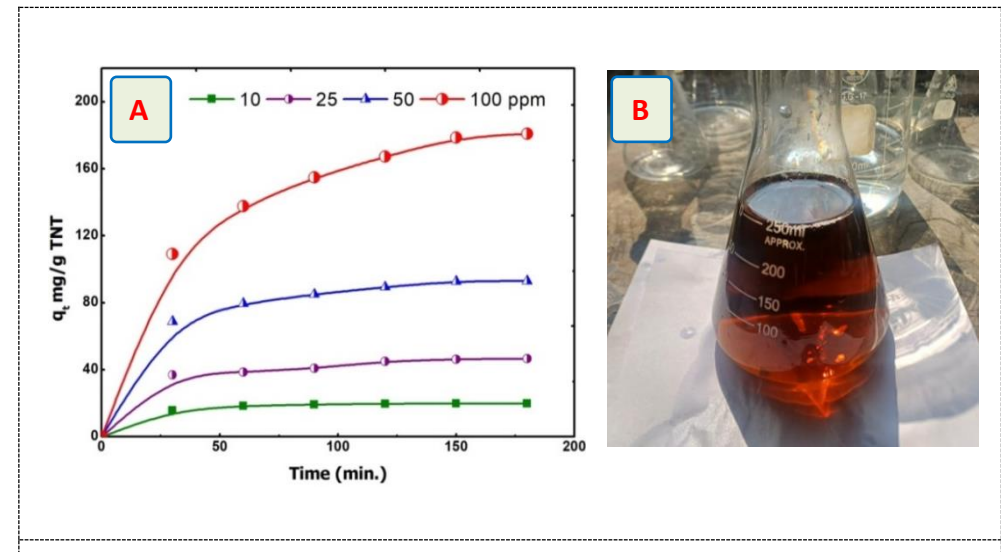


Figure 3. a) Effect of different concentrations from TNT adsorbed on GO b) A photograph of prepared GO.

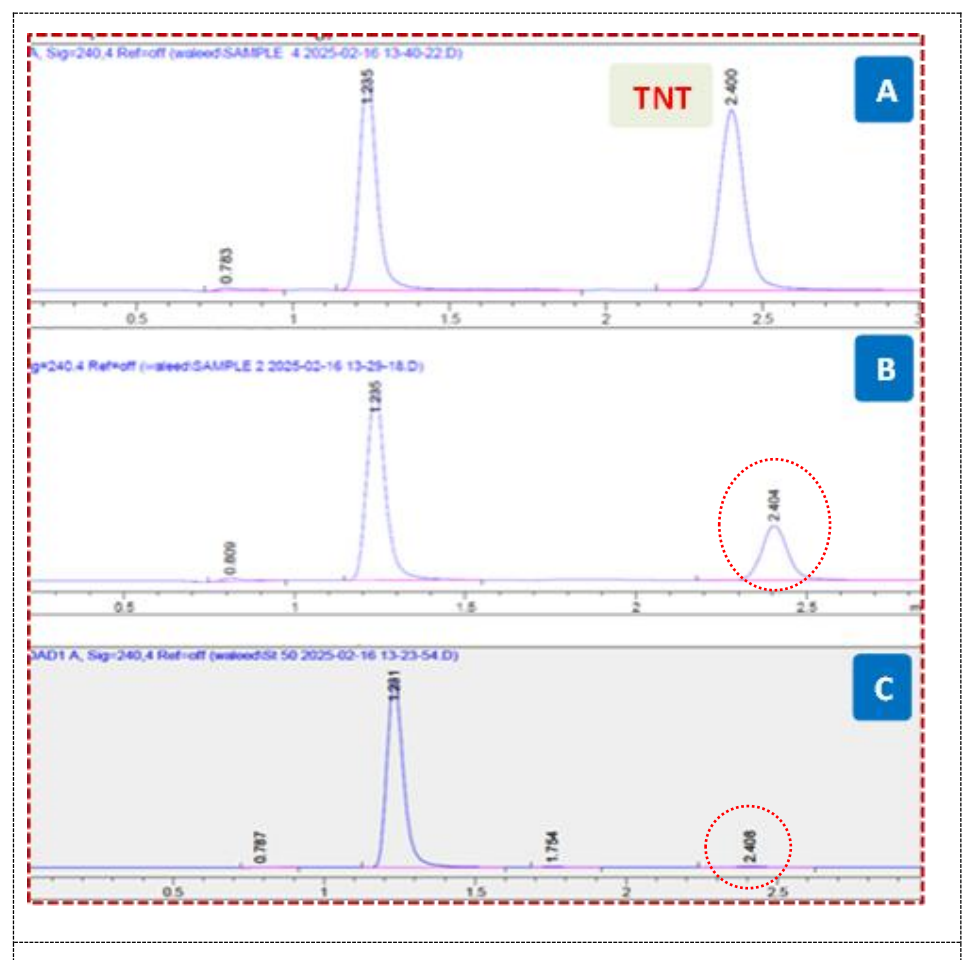


Figure 4. The HPLC results of TNT adsorbed on GO a) before adsorption b) start to adsorbed c) final removal.

3.2.3 Effect of initial pH.

The pH greatly impacts adsorbent efficacy, making it an essential regulatory factor. The adsorption of TNT onto the GO surface is affected by pH, as seen in Figure 5b (0.5 g/L adsorbent and 100 ppm TNT). The adsorption capacities of TNT for pure GO were 161.2, 180.8, and 147.1 mg/g at pH levels of 4, 6, and 9, respectively. The adsorption capacity diminished by 11% when the pH was reduced from 6 to 4 and by 18.3% when the pH was elevated from 6 to 9. The removal efficiency is low because there is a lot of competition for the adsorption sites between TNT and many H+ ions. As the pH levels transitioned from acidic to neutral, the efficacy of TNT removal swiftly increased to its peak performance. The enhanced adsorption capacity results from interactions between the target TNT compounds and the functional groups that gradually lose protons. Soluble OH-TNT complexes have difficulty adhering to GO due to their predominance in solution at elevated pH levels. The findings of this analysis are wholly consistent with those of the prior study [18].

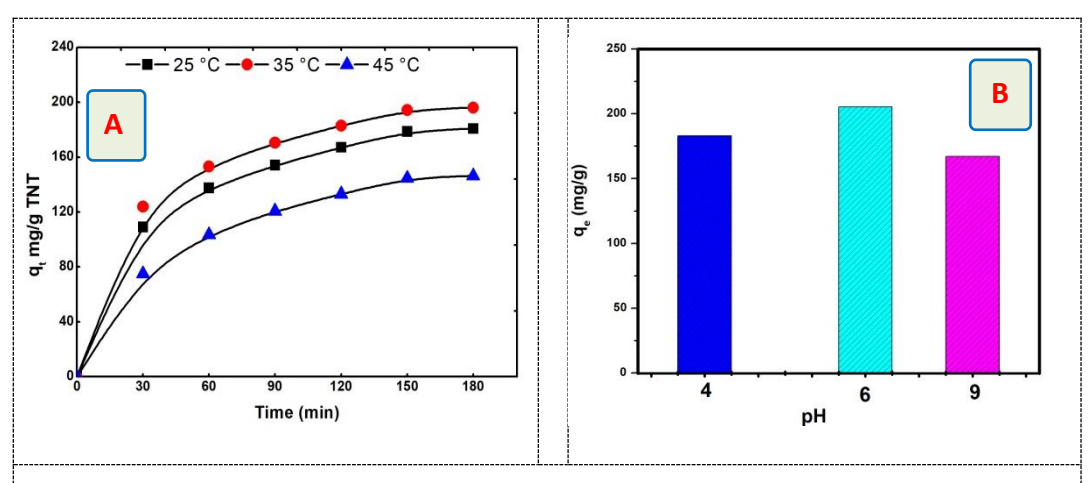


Figure 5: A) Effect of temperature on adsorption capacity of Cobalt GO-TOPO at pH 6. B) Effect of pH on adsorption capacity at room temperature.

4. Conclusion

This work was mainly focused on the production of graphene oxide (GO) using a modified improved Hammer method. The TEM, FTIR, XRD, and Raman spectroscopies were employed to examine the generated graphene oxide. TNT was successfully recovered from the water using the GO method. We conducted a study to explore the impact of temperature, pH, and contact time duration on the adsorption process. The HPLC study showed that graphene oxide was excellent at removing most nonpolar organic pollutants, especially 2, 4, and 6-trinitrotoluene. The results demonstrate that the ideal pH and temperature for eliminating TNT from water are 6.0 and 35 degrees Celsius, respectively. The result revealed that the maximal adsorption capacity of GO was approximately 180.8 mg/g.

References

- [1] D.H.K. Reddy, S.-M. Lee, Advances in colloid and interface science, 201 (2013) 68-93.
- [2] S.M. King, University of New Orleans, 2012.
- [3] A. Yadav, M.O. Aquatar, R.J. Krupadam, (2024).
- [4] X. Zhang, Y.-m. Lin, X.-q. Shan, Z.-l. Chen, Chemical Engineering Journal, 158 (2010) 566-570.
- [5] S. Chatterjee, U. Deb, S. Datta, C. Walther, D.K. Gupta, Chemosphere, 184 (2017) 438-451.
- [6] M. Zhang, G.-h. Liu, K. Song, Z. Wang, Q. Zhao, S. Li, Z. Ye, Chemical Engineering Journal, 259 (2015) 876-884.
- [7] P. Hu, Y. Zhang, F. Lv, X. Wang, F. Wei, X. Meng, S. Jiang, Water, Air, & Soil Pollution, 225 (2014) 1-10.
- [8] H. Mangal, A. Saxena, N. Shukla, P. Rai, A. Rawat, V. Kumar, V. Gupta, M. Datta, Water Science and Technology, 75 (2017) 716-726.
- [9] Bharti, I. Khurana, A.K. Shaw, A. Saxena, J.M. Khurana, P.K. Rai, Water, Air, & Soil Pollution, 229 (2018) 1-16.
- [10] W.F. Khalil, A. Agha, R. Rayan, Journal of Physics: Conference Series, IOP Publishing, 2022, pp. 012014.
- [11] S. EPA, Environmental Protection Agency, 8330 1-21.
- [12] X. Wang, Z. Chen, S. Yang, Journal of Molecular Liquids, 211 (2015) 957-964.
- [13] W.F. Khalil, F. Mubarak, A. Agha, R. Zaky, F.A. Kamel, The International Conference on Chemical and Environmental Engineering, Military Technical College, 2024, pp. 1-8.
- [14] C.J. Madadrang, H.Y. Kim, G. Gao, N. Wang, J. Zhu, H. Feng, M. Gorring, M.L. Kasner, S. Hou, ACS applied materials & interfaces, 4 (2012) 1186-1193.
- [15] H. Chen, D. Shao, J. Li, X. Wang, Chemical Engineering Journal, 254 (2014) 623-634.

- [16] W.M. El Rouby, A.A. Farghali, M. Sadek, W.F. Khalil, Journal of Inorganic and Organometallic Polymers and Materials, 28 (2018) 2336-2349.
- [17] C. Wang, H. Luo, Z. Zhang, Y. Wu, J. Zhang, S. Chen, Journal of Hazardous materials, 268 (2014) 124-131.
- [18] Y. Cai, X. Wang, J. Feng, M. Zhu, A. Alsaedi, T. Hayat, X. Tan, Environmental Pollution, 249 (2019) 434-442.